Live 3D Guidance in Endovascular Procedures

A showcase of patient studies illustrating the benefits of advanced live 3D guidance tools in a busy day-to-day clinical practice.

BY ATUL GUPTA, MD, AND ALESSANDRO G. RADAELLI, PhD

Today's endovascular interventionists must be skilled with the latest device and imaging technology to best treat their patients. An accurate morphological assessment of blood vessels and their relationship with interventional devices is essential to the management of vascular lesions, and digital subtraction angiography (DSA) has had a central role in the deployment of interventional procedures. High resolution, the ability to selectively evaluate individual vessels, and the access to direct physiological information make DSA a cornerstone technology in endovascular procedures. The addition of three-dimensional rotational angiography (3D RA) and flat panel detector technology have further contributed to greater diagnostic accuracy, faster procedures, and improved outcomes.[1-4] In particular, 3D reconstructions from rotational angiograms have overcome limitations of two-dimensional (2D) imaging such as false vascular foreshortening due to projection angle and vessel obscuration due to overlying vessel or bone. These 3D reconstructions are now routinely used to reveal complex vascular relationships. Major developments in hardware and software of x-ray angiographic systems have significantly increased the usability of this technique, and 3D reconstructions are now performed and available for analysis and manipulation in real-time. The availability of 3D reconstructions also carries along a wealth of 3D tools that can improve current procedural workflows starting from disease assessment to treatment evaluation through navigation and treatment planning.

The use of 3D RA and associated tools in endovascular procedures is, however, not yet common practice. Although evidence of the clinical benefit and reduction in radiation exposure to patients and staff following the use of 3D RA has been extensively reported for vascular

> "The addition of 3D RA and flat panel detector technology have further contributed to greater diagnostic accuracy, faster procedures, and improved outcomes."

lesions of the neck and brain,[5-10] there is not enough information in the literature on how the use of 3D tools can improve the (peripheral) vascular procedural workflow with potentially no changes (or reduction) to radiation and contrast administration. This article provides a showcase of minimally invasive endovascular applications in which the availability of 3D tools was distinctively beneficial to achieve effective disease management in a busy day-to-day clinical practice.

MATERIALS AND METHODS

The interventional radiology department at Paoli Hospital performs approximately 5,400 procedures per year, covering the full spectrum of vascular and nonvascular interventions. In order to provide a suitable range of endovascular procedures, 10 patients were selected retrospectively from a data pool of more than 200 subjects treated between 2006 and 2007 with clinically indicated rotational angiography. The clinical indication was made by the interventional radiologist on a per-case basis based on his judgment as to whether the 3D tools would help in problem solving or clarification of anatomy, offer any potential time savings, possibly reduce contrast or x-ray dose to the patient, or uncover a suspected hidden lesion. All rotational examinations
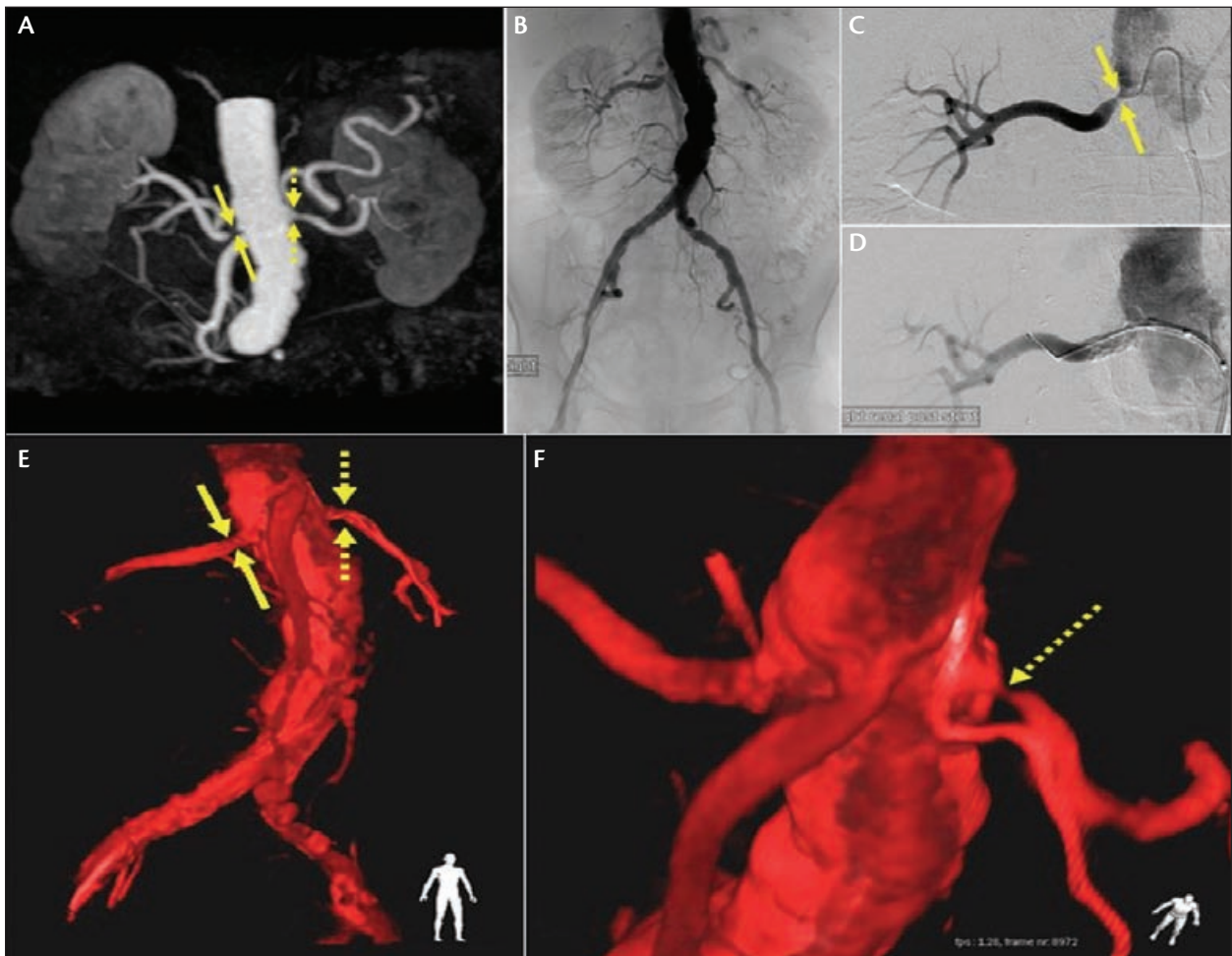
Figure 1. A renal artery stenosis in an 81-year-old woman. The patient was referred for treatment after failed medical management of hypertension. Preprocedure contrast-enhanced MR angiography showing a tight ostial stenosis of the right renal artery (arrows) and a patent left renal artery (dashed arrows) (A). Repeat anteroposterior (AP) arteriogram of descending aorta and iliac arteries confirming the right renal artery stenosis (B). Selective DSA image of the right renal artery showing stenosis (arrows) at the origin of the vessel (C). Selective DSA image of the right renal artery showing successful stenting (D). AP view of the 3D RA reconstruction showing unremarkable left (dashed arrows) renal artery and the good poststent appearance of the right renal artery (arrows) (E). Oblique view (right anterior oblique [RAO] = -6°, cranial [CRAN] = -52°) revealing the presence of two overlapping vascular segments on the left side, which hide a very tight stenosis of the left renal artery (dashed arrow) (F). The lesion was further confirmed with pullback pressure measurements. After stenting of the left renal artery, hypertension was successfully controlled.

were performed on a Philips Allura Xper FD20 system (Philips Medical Systems, Best, The Netherlands) using an automated "two-button" 3D acquisition process. Contrast material was injected during acquisition through a catheter placed into the vascular territory of interest. A total of 120 frames were obtained during a 240° rotation for a total scan time of 4 seconds. The frames were automatically sent to a dedicated workstation where 3D reconstructions with a field of view of 25 X 19 X 25 cm^3 and a matrix size of 128^3 were generated in real time. These real-time 3D images were displayed in the procedure room, alongside or even embedded within the fluoroscopic images. All 3D analyses were performed live by the physician who carried out the examination.

The 3D reconstructions were used to visualize the vascular anatomy from multiple angles, select the optimal working projection, and simultaneously synchronize the position of the C-arm. This is now possible because modern workstations are fully integrated with
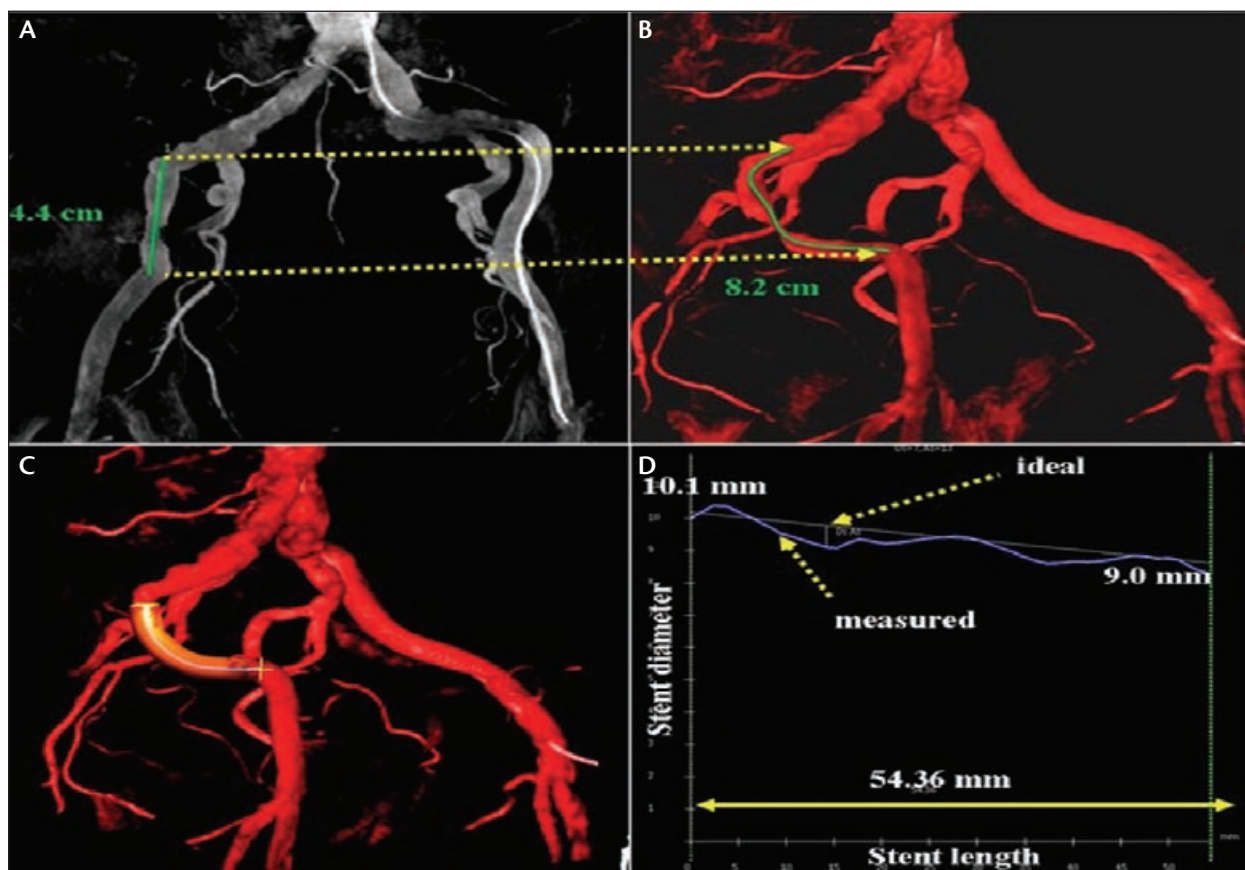
Figure 2. An external iliac artery stenosis in a 79-year-old man. AP view of aortoiliac arteriogram (A). Lateral view (RAO = -38°, CRAN = -4°) of a 3D RA reconstruction better showing the vascular morphology (B). Had the stenosis extended over a longer segment, stent sizing based on 2D imaging would have been particularly unfavorable. The same view of the posttreatment 3D RA reconstruction and results of virtual interventional tools, used in this case to analyze the stented vascular segment (C). Quantitative information provided by the advanced vascular analysis tool (D). The good outcome of the stenting procedure is shown by a satisfactory stent opening throughout the lesion and by a smooth transition from proximal to distal ends (blue line) also when compared with an ideal linear transition provided by the software (yellow line).

the acquisition system and directly coupled with the C-arm geometry. The synchronization could also be exploited to achieve live 3D navigation through the real-time superimposition of live fluoroscopy images on a surface-rendered 3D reconstruction (Dynamic 3D Roadmap, Philips Medical Systems). Changes to the live fluoroscopy images after adjustment of x-ray/detector distance, position, and/or magnification are transferred to the 3D reconstruction so that the matching is maintained throughout the procedure. When available, preinterventional computed tomography (CT) and magnetic resonance (MR) scans could also be transferred to the workstation, matched with 2D live fluoroscopy, and used for 3D navigation.

Three-dimensional reconstructions were further processed using quantitative analysis tools. Vessel size

and stenosis grading were measured in 3D using advanced vascular analysis and virtual stenting functionalities, which provide an accurate delineation of local vascular diameter and length and a simulation of stent placement that facilitates the selection of commercially available stents. In the case of aneurysms, a built-in, computer-assisted aneurysm analysis tool was used to automatically detect significant vascular dilatations and obtain quantitative information such as aneurysmal volume and neck size.

For procedures requiring intraoperative visualization of soft tissues, CT-like 3D reconstructions were acquired using the XperCT (Philips Medical Systems) technique. XperCT is an additional rotational acquisition mode performed over a scan range of 240° resulting in 310 frames and a total scan duration of 10 seconds. When required,

XperCT and 3D RA were matched to visualize interventional devices and soft tissues along with contrast-filled vessels and assess treatment completion.

CLINICAL RESULTS

Vascular Stenoses

Three-dimensional imaging is useful in the assessment and grading of vascular stenoses. Not only can it provide a view of the anatomy from angles not achievable with 2D imaging, but 3D imaging also helps in the detection of hidden stenoses not visible in 2D projections and other diagnostic images (Figure 1).

The benefits of 3D information also extend to a better estimation of the required stent characteristics. For instance, when performing iliac stenting, most interventional radiologists are trained to acquire an anteroposterior (AP) aortoiliac arteriogram and two additional oblique angiographic projections. Due to the high tortuosity of the external iliac arteries, the use of conventional 2D images and "eyeballing" may lead to underestimation of the length of the vessel and ultimately to incorrect stent sizing. By using 3D RA and quantitative tools, the radiologist can accurately evaluate the extension and grading of the stenosis and select the right stent from the start, thus avoiding the need of overlapping stents with the associated extra costs and risks of recurrent stenosis (Figure 2).

Trauma

Three-dimensional imaging provides detailed anatomical information that assists decision making for emergency and trauma patients. Three-dimensional information can be used to elucidate the relationship between foreign bodies and vascular structures and support/exclude the need for complex surgical procedures (Figure 3). In this case, 3D RA was superior to high-resolution multiplanar CT visualization, film radiography, and conventional 2D venography in providing quick, optimal anatomical viewing and facilitating timely and confident decisions.

Visceral Aneurysms

Accurate imaging information on volume, location, neck size as well as the relationship with parent vessel and side branches is essential in the diagnostic assessment and treatment planning of aneurysms. Often, this type of information cannot be obtained—neither from
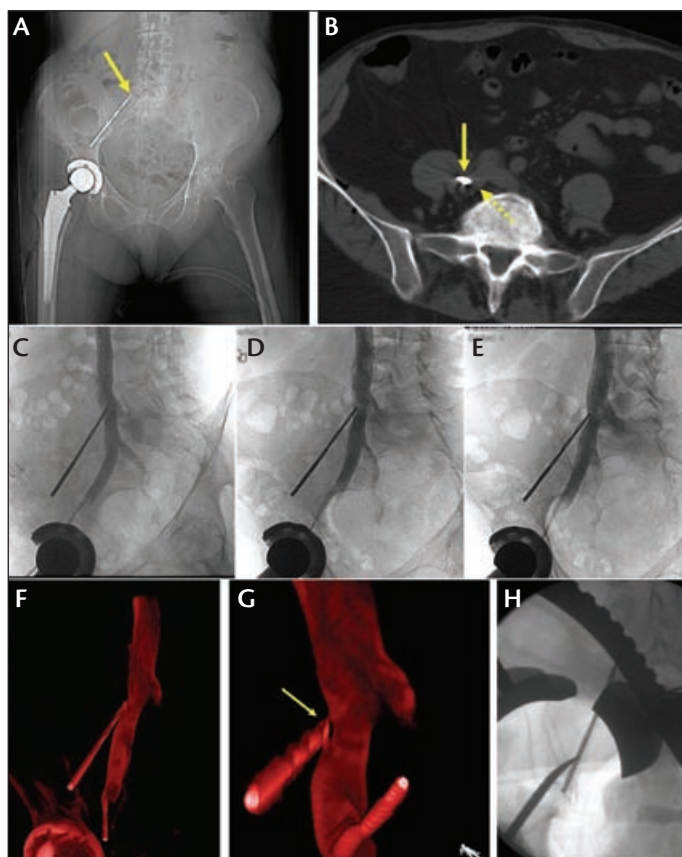

Figure 3. An accidental drill bit penetration in the pelvis of 75-year-old woman during hip replacement. Radiography showing the location of the broken drill bit (arrow) in a precarious area of the pelvis (A). Axial view of subsequent CT scan (B). The head of the drill bit (arrow) appears to have penetrated the common iliac vein (dashed arrow). Two-dimensional venograms acquired at several different oblique angles further suggest penetration of the drill bit into the iliac vein (C through E). A 3D rotational venogram showing the relationship between the prosthesis' acetabular head, drill bit, and common iliac vein (F). Magnified and rotated view (RAO = 60°, caudal = 57°) revealing a tissue plane between the tip of the drill bit and the iliac vein (arrow), conclusively ruling out vessel perforation, contrary to CT and 2D venogram findings (G). This obliquity was impossible to achieve with 2D venography. Fluoroscopic image acquired during subsequent intervention (H). The drill bit is simply grabbed and pulled out with a hemostat without any resulting complication. Three-dimensional imaging saved the patient a complex retroperitoneal dissection and vascular surgery.

2D DSA due to complex angles required to view the aneurysm neck nor from CT angiography (CTA) and magnetic resonance angiography (MRA)—because of inadequate spatial resolution, especially for small branch vessels. CTA and MRA typically provide a spatial resolution greater than 0.4 to 0.5 mm, whereas a resolution of 0.1 to 0.2 mm can be expected from 3D RA.
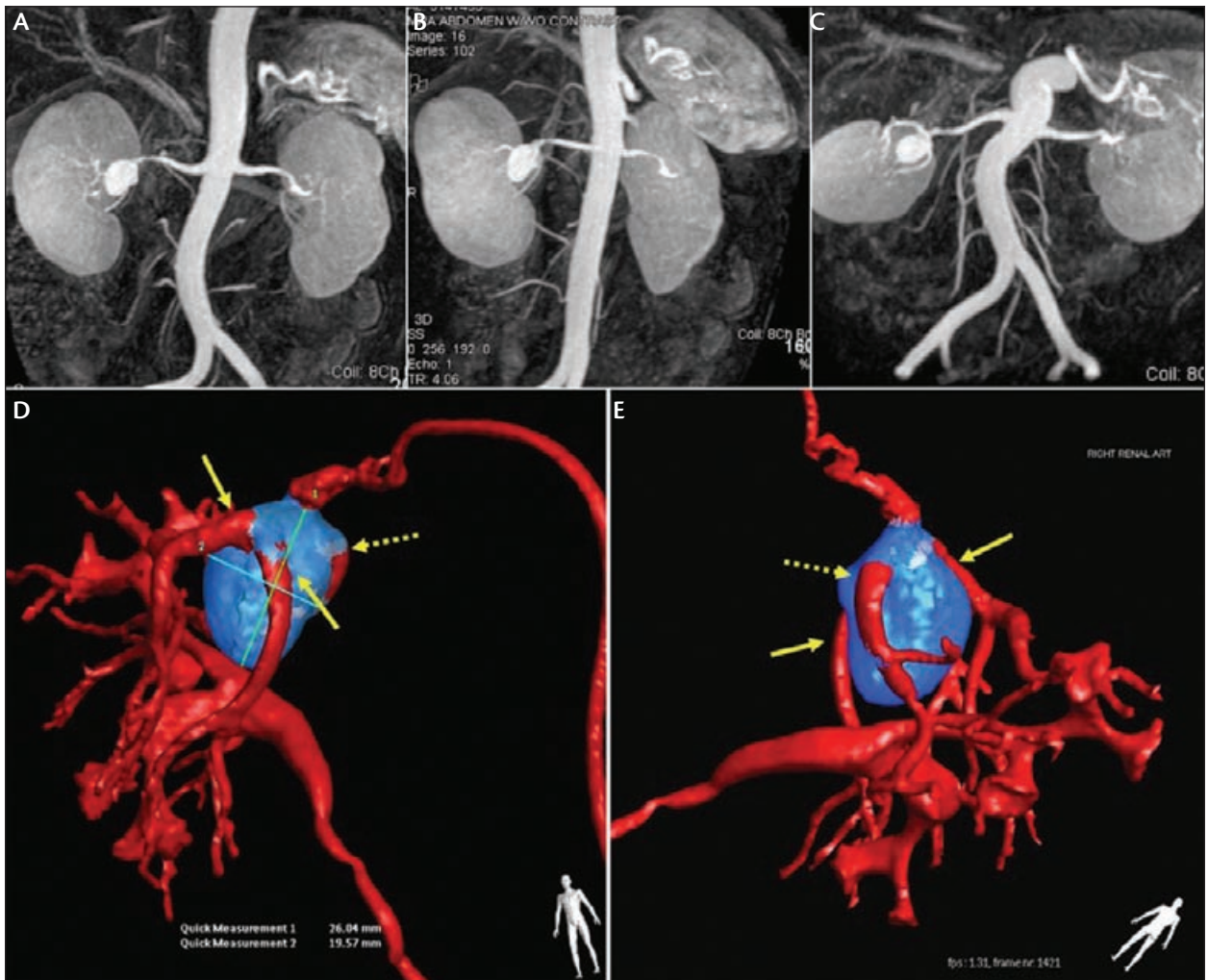
Figure 4. A renal artery aneurysm in a 55-year-old man (A through C). Selected views of diagnostic 3D MRA showing an aneurysm of the right renal artery. Although spatial resolution is inadequate for confident neck localization and sizing, the image (C) shows optimal viewing angle to best define the aneurysm neck. A similar view with 2D DSA would not be achievable because it would have required a very steep craniocaudal oblique angle. Selective 3D RA reconstruction of vascular aneurysm after the injection of 8 mL of contrast using a catheter placed into the right renal artery (captured on the image). The relationship between the aneurysm and feeding vessels could be visualized at any angle. Surface rendering of the 3D RA reconstruction (D). The aneurysm is isolated and shaded in blue using an automatic detection algorithm implemented in the computer-assisted aneurysm analysis tool. The visualization helps in the quantification of aneurysm size and shows how all three vessels feeding the kidney (arrows) arise from the aneurysm sac. An additional view offering a better depiction of the posterior vessel branch (dashed arrow) (E). The patient was referred, along with a 3D RA video file, to a transplant surgeon for bench surgery and autotransplantation as endovascular repair with coils/covered stents was not a good option.

Renal arteries are common locations of vascular aneurysms, and appropriate anatomical information is critical. For example, incorrect deployment of endovascular coils due to underestimation of neck size may lead to nontarget embolization with possible kidney infarction. Three-dimensional RA offers high spatial resolution and can achieve a detailed 360° view of the vessels of interest. Computer-assisted aneurysm analysis tools can also be used to automatically define the aneurysm sac, calculate its dimensions, and analyze its relationship with the surrounding vessels, facilitating both diagnostics and interventional planning (Figure 4). In this case, a video file of the 3D RA reconstruction was supplied to transplant surgeons prior to surgery to help them plan the best method of vascular repair during bench surgery (autotransplantation). This resulted
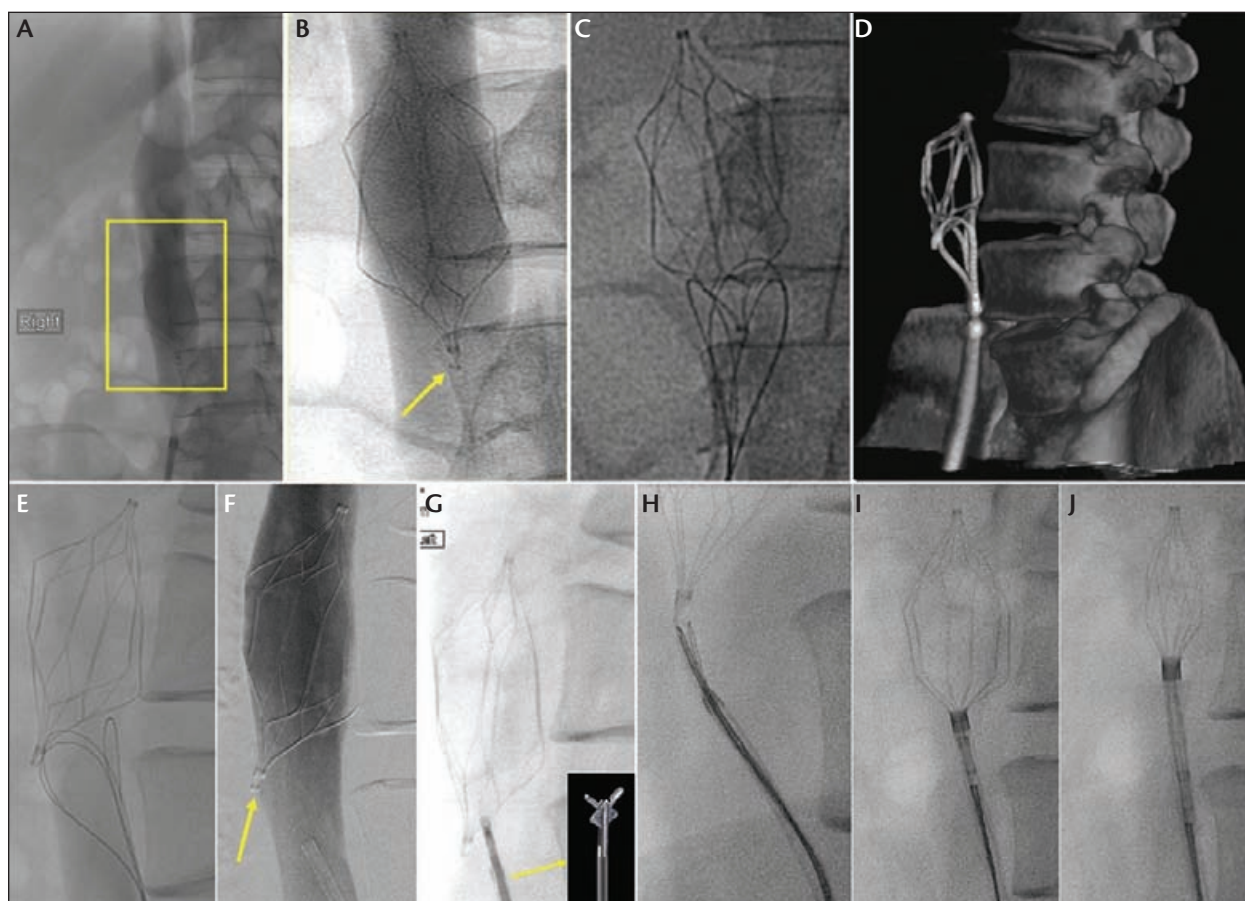
Figure 5. An IVC filter removal in a 44-year-old man. Two-dimensional AP venography showing the IVC and OptEase IVC filter (Cordis Corporation, Warren, NJ) (A). A magnified view of the filter suggests the correct positioning of the hook (arrow) in the middle of the vein's lumen (B). Two-dimensional AP fluoroscopy showing an unsuccessful attempt to capture the filter's hook using a snare (C). A 4-second 3D RA reconstruction showing the spine, tilted IVC filter, and its relationship with the snare used to capture the hook (D). Lateral (84°) 2D fluoroscopy optimally showing filter tilting (E). The exact lateral angle was selected from the 3D image. Lateral (84°) 2D digital subtraction venography further exposing the relationship between the filter and the IVC (F). The filter is not only tilted, but the hook (arrow) is also embedded into the vessel wall. Snare retrieval would have been physically impossible and would have inevitably led to numerous unsuccessful attempts. An endovascular forceps (shown inset) is advanced and grasps the filter's struts (G). The hook is gently brought back into the vessel lumen. Fluoroscopic sequence showing subsequent filter removal (H though J).

in minimizing the ischemia time of the explanted native kidney during repair, because much of the repair planning could be done prior to surgery.

Inferior Vena Cava Filter Removal

Retrievable inferior vena cava (IVC) filters are increasingly being used to prevent pulmonary embolism. Several weeks or months after implantation, patients are typically brought back for filter removal. Most retrievable IVC filters incorporate a "retrieval hook" that is used to capture the filter, and these filters are designed in a manner to avoid tilting and ensure correct positioning of the hook in the middle of the IVC.

When properly placed, the filter is typically removed within minutes with a snare and sheath.

Often, the removal process requires several snare attempts and lengthy fluoroscopic exposures. Even symmetric filters, while appearing untilted in standard 2D venograms, may hide a significant degree of tilt, which is often revealed with unusual projection angles.[11] Our approach is therefore to routinely perform a rapid, 4-second 3D RA at the start of the procedure to achieve a fast and confident removal, even in complex cases. A single acquisition provides all the necessary information to quickly and accurately visualize the filter and the IVC, plan the appropriate removal
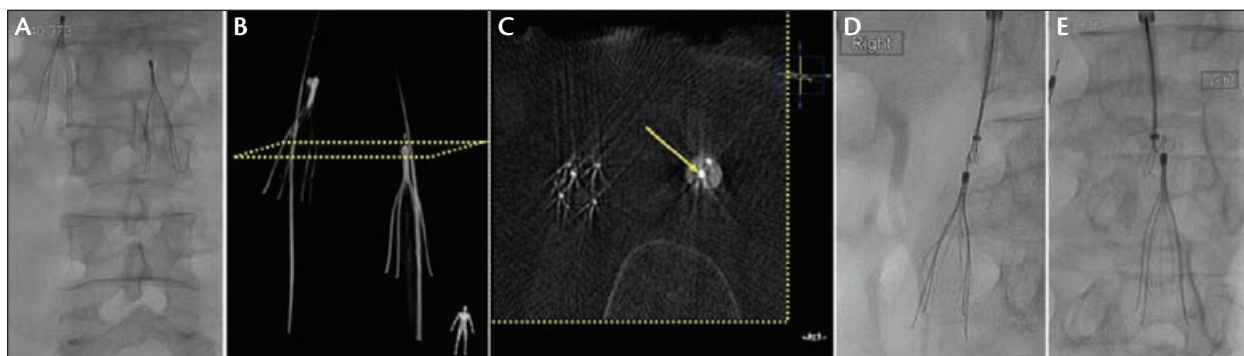
Figure 6. Dual retrieval of bilateral IVC Celect filters (Cook Medical, Bloomington, IN) (first reported worldwide) in a 58-year-old man with duplicated IVC. Two-dimensional AP fluoroscopy of the patient's abdomen showing IVC filters (A). Volume rendering of pretreatment 3D rotational venography (B). The intensity threshold value was selected so as to optimally visualize the filters only. The virtual plane (in yellow) corresponds to the location of the axial slice (C). Selected axial slice of real-time CT-like reconstruction from 3D venography showing the location of the left filter's hook (arrow) in the middle of the IVC (C). Two-dimensional fluoroscopy during removal of the right filter (D). Two-dimensional fluoroscopy during removal of the left filter (E).

approach, and select the optimal working projection, often becoming a significant time saver (Figure 5).

The possibility of visualizing the rotational acquisition as a "CT-like" multiplanar reconstruction further facilitates the analysis of the hook positioning with respect to the IVC lumen, thus making the removal process simple and fast (Figure 6).

Vascular Malformations

Endovascular treatment of arteriovenous malformations (AVMs) can be quite complex. Although diagnostic multiplanar 3D CTA or MRA images are valuable for AVM detection, they do not offer adequate spatial resolution to precisely analyze the "spaghetti-like" arterial supply and determine the optimal angle of approach for each feeding vessel. Three-dimensional RA offers more detailed anatomical information that enables the radiologist to untangle the tangled web of vessels surrounding the AVM, choose the angles to selectively show the feeders, and define treatment approach and chronology.

A comprehensive treatment plan based on 3D RA is achieved with a single run and helps to minimize the number of 2D DSA and fluoroscopic images required during treatment. The minimization of iodinated material is particularly important for patients affected by renal AVMs because renal function may be impaired due to preparenchymal shunting of blood, with resultant bypassing of renal filtration. Additionally, further kidney injury may result from imprecise or nontarget embolization. Thus, optimal viewing angles are critical. The use of 3D imaging is particularly beneficial in these patients and helps us to achieve a favorable balance

> "Three-dimensional imaging provides detailed anatomical information that assists decision making for emergency and trauma patients."

between contrast minimization, optimal viewing, and a prompt recovery of kidney function (Figure 7).

Accurate 3D imaging plays a significant role for malformations affecting the uterine arteries. Uterine AVMs are particularly complex and tortuous, and, even if the proximal uterine artery is correctly embolized, parasitization and collateral vessels such as the ovarian artery may rapidly take over and continue feeding the malformation. Should the malformation be inadequately embolized, uterine expansion during pregnancy may lead to vessel rupture and to life-threatening hemorrhage for the mother. The availability of 3D RA reconstructions is therefore essential to quickly identify the nidus, unravel the intricate vascular configuration of the feeding vessels, select the optimal working projections to access all feeding vessels, and achieve a complete embolization (Figure 8).

Uterine Fibroid Embolization

Uterine fibroid embolization (UFE) is an important application making use of 3D imaging.[12] UFE is performed by introducing small embolic particles into uterine arteries feeding the fibroid, resulting in fibroid shrinkage. The imaging technique of choice for this procedure is conventional angiography. Most interventional
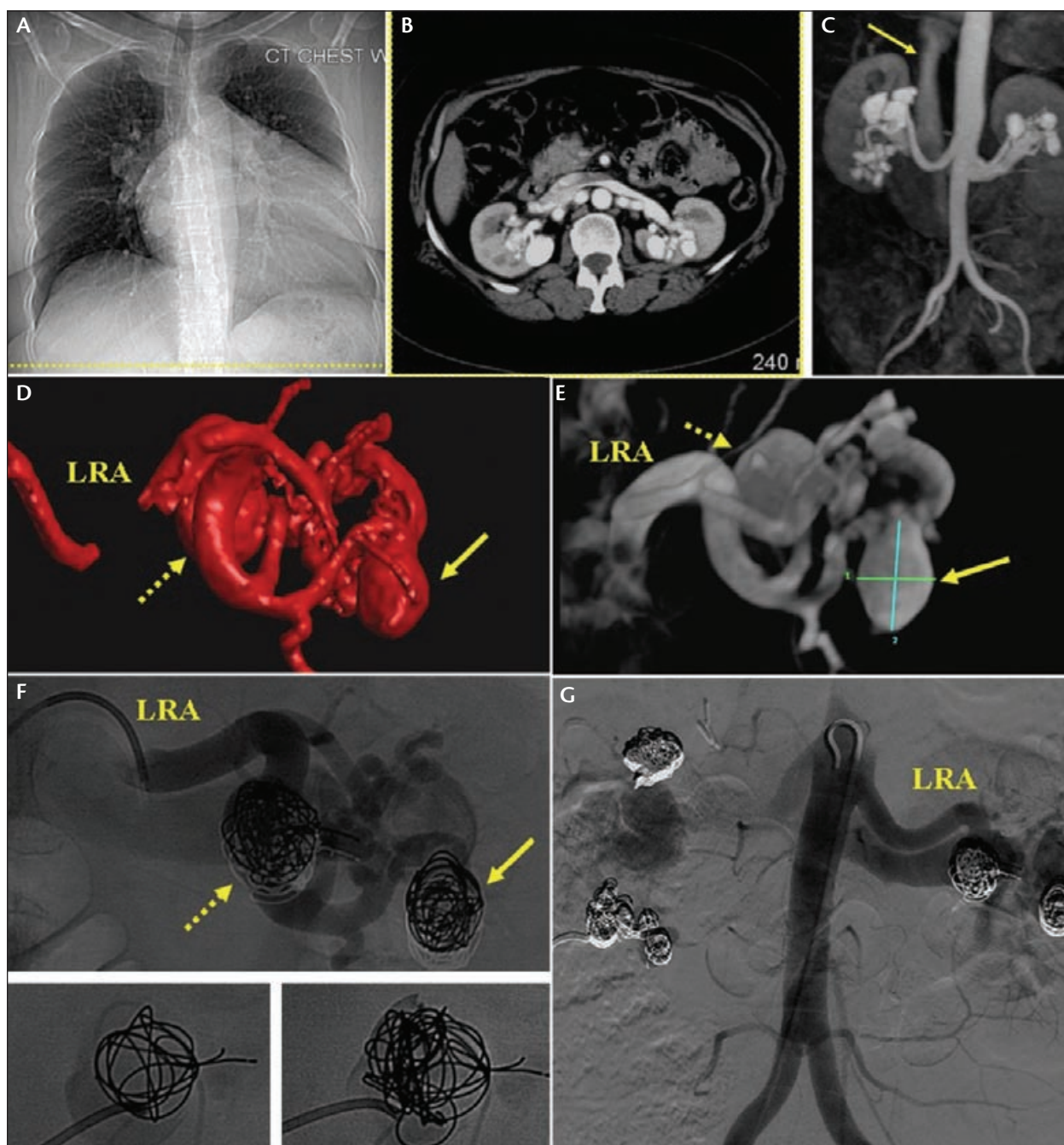
Figure 7. Bilateral renal AVMs discovered in a 69-year-old woman with congestive heart failure (CHF) who presented with severe shortness of breath and suspected pulmonary embolism (PE). An AP view of chest showing severe cardiomegaly (A). The last axial slice obtained from the CT PE study (dashed line [A]) shows abnormal appearance of the renal arteries, suggesting the presence of bilateral AVMs (B). MRA of renal arteries confirming AVMs with early enhancement of the renal veins and IVC (arrow) suggesting high-flow arteriovenous shunting (C). AP view of selective 3D RA surface rendering of the left renal artery (LRA) showing complex AVM with outpouching aneurysms prior to embolization (D). Location and feeding vessels of the AVM (arrows) are nicely exposed. Oblique view of 3D RA grayscale rendering used for aneurysm measurement and for selection of angles needed to access the feeding vessels (E). Embolization performed with angles selected from 3D RA (F). Posttreatment 2D AP DSA (G). Patient's fatigue and shortness of breath resolved after treatment, with an improvement in the kidney function (creatinine dropped from 1.9 to 1.5 mg/dL) due to improved renal parenchymal perfusion.
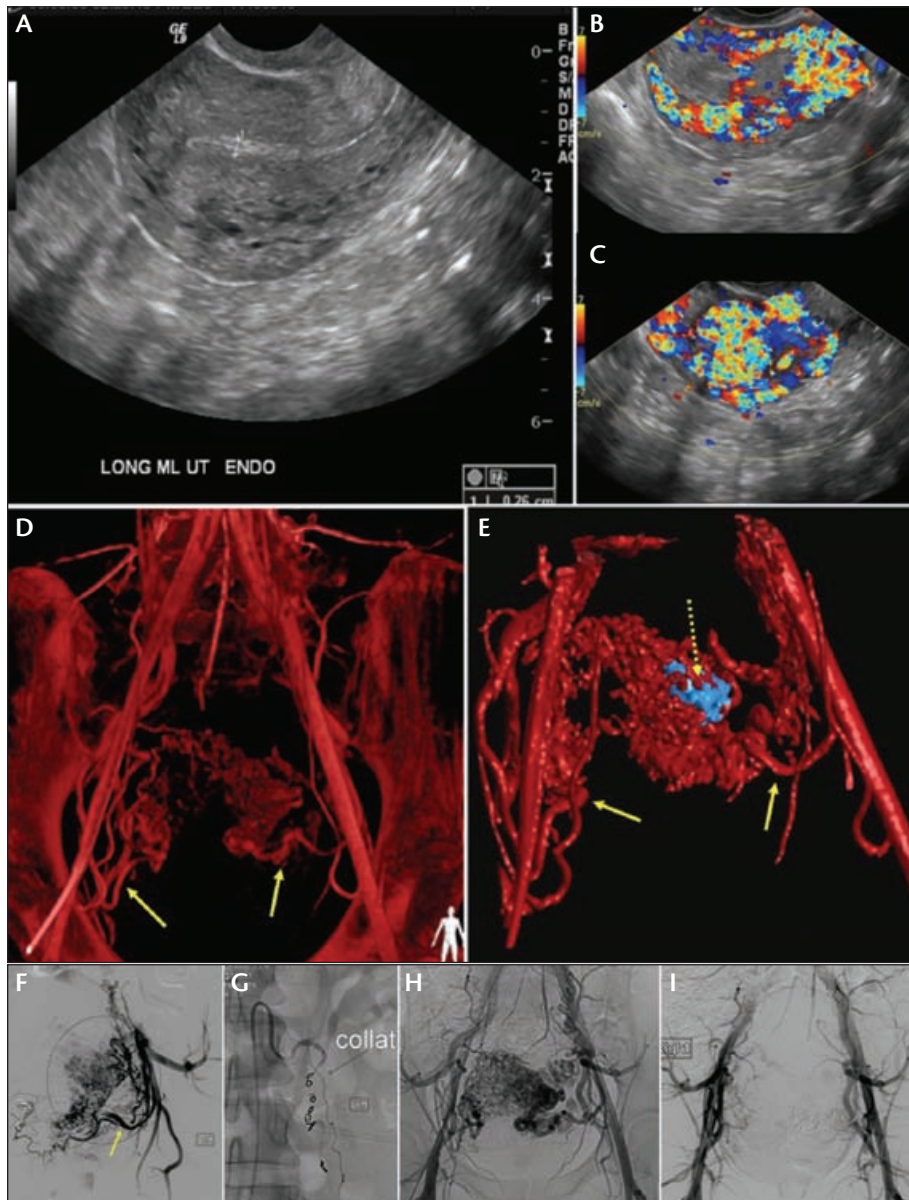
Figure 8. A uterine AVM in a 26-year-old woman with a history of gestational trophoblastic disease (treated with dilatation and curettage 1 year earlier) presenting with pelvic pain. Patient desires pregnancy. Longitudinal grayscale endovaginal ultrasound of uterus (A). Longitudinal color Doppler ultrasound showing marked diffuse uterine hypervascularity (B and C). Subsequent MRA examination confirmed a large uterine AVM. AP view of 3D RA reconstruction of uterine vessels revealing complex malformation (D). The uterine arterial supply (arrows) was satisfactorily identified and could be inspected at any angle. Surface rendering of 3D RA reconstruction (E). The AVM nidus is depicted in blue after automatic detection with the advanced aneurysm analysis tool (dashed arrow). Angiography of left uterine artery (arrow) during embolization (F). Angiography of parasitized left ovarian artery following embolization (G). Pretreatment 2D AP DSA (H). Posttreatment 2D AP DSA showing complete AVM embolization after treatment of right and left uterine and left ovarian arteries (I). The patient became pregnant a few months after treatment and ultimately delivered a healthy baby with no complications.

radiologists perform abdominopelvic aortography with additional, randomly chosen oblique selective internal iliac angiograms. The angle selected is quite variable from operator to operator and is performed in hopes of localizing the origin of the uterine artery and to produce a road map to guide superselective catheterization of this vessel. While occasionally this randomly selected angle may be adequate, very often additional angiographic road maps in other angles are performed to successfully show the origin of the uterine artery. This increases procedural radiation dose, contrast administration, and procedure time. Our approach is instead to acquire one 3D RA at the beginning of the procedure using a distal aortic contrast injection to produce a 360° view of the feeding arteries. A single 3D RA 4 second acquisition with near-instant reconstruction is then used to select the optimal projection to show the origins of the uterine arteries. A 3D dynamic road map can then be used to swiftly access the feeding arteries with no need for any additional contrast or DSA runs prior to the embolization (Figure 9).

Transarterial Chemoembolization

The combination of live 3D tools is particularly valuable in transarterial chemoembolization (TACE)
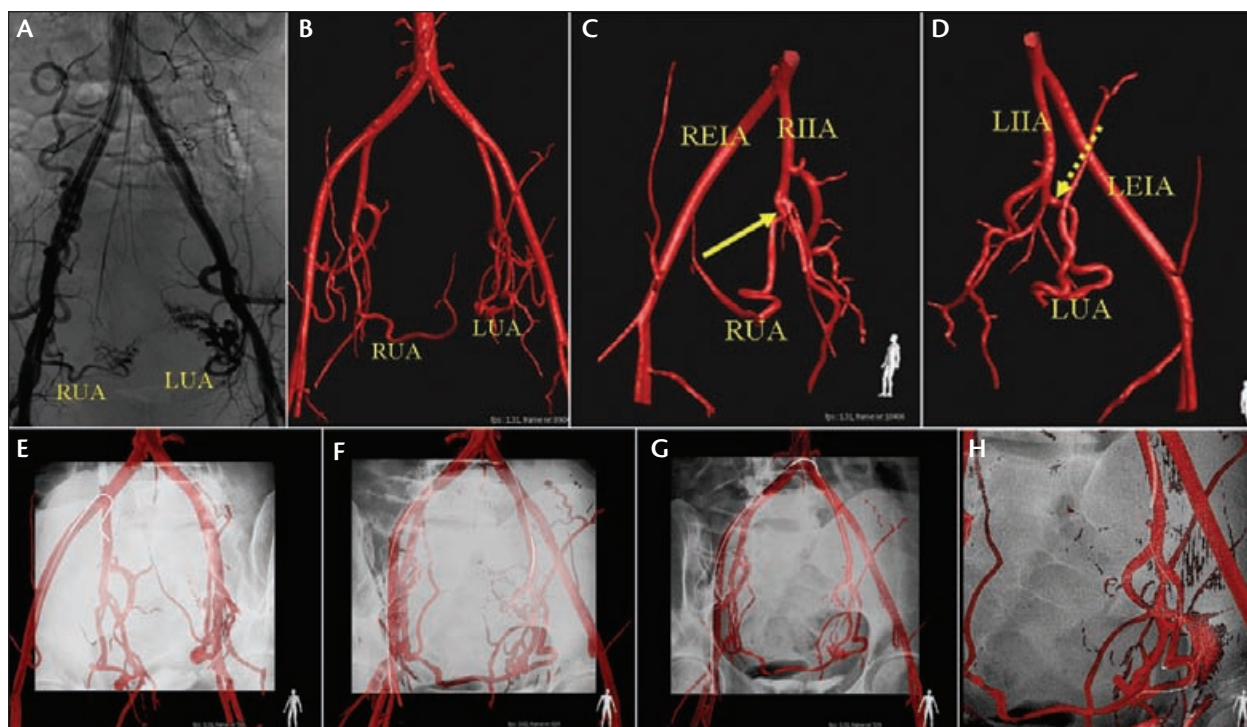
Figure 9. A uterine fibroid embolization in a 41-year-old woman. Two-dimensional aortoiliac angiogram showing bilateral supply of the uterine arteries feeding the fibroid (A). AP view of 3D RA surface rendering obtained after aortic injection of 30 mL of iodinated contrast (B). Oblique view of cropped 3D RA surface rendering showing branches of the right external and internal iliac arteries (REIA and RIIA, respectively) used to identify the origin (arrow) of the right uterine artery (RUA) (C). Oblique view of cropped 3D RA surface rendering showing branches of the left external and internal iliac arteries (LEIA and LIIA, respectively) used to identify the origin (dashed arrow) of the left uterine artery (LUA) (D). Snapshots recorded during live 3D navigation with the Dynamic 3D Roadmap (E through H). A single 3D reconstruction was used throughout the embolization procedure. The magnification and projection angle of the live fluoroscopy were automatically transferred to the 3D reconstruction so as to preserve their matching. The blending of the two types of data could also be controlled to, for example, highlight vascular landmarks or boost catheter visualization.

procedures. Starting from a 3D RA scan, accurate anatomical information is available to identify the vessels feeding the tumor and plan the treatment approach. The 3D RA volume can also be registered and fused with diagnostic CTA or MRA to obtain valuable multimodal visualizations of feeding vessels and tumors. During navigation, the 3D RA volume can then be matched with live 2D fluoroscopy to achieve a Dynamic 3D Roadmap and a smooth catheter placement into the feeding vessels. Finally, soft tissue information obtained with the XperCT protocol can be used to confirm treatment completion by comparison with pretreatment CTA or MRA. The availability of CT-like imaging in the interventional suite enables the interventionist to promptly tackle possible tumor residuals and improves the clinical workflow eliminating the need of moving the patient to a CT unit (Figure 10).

DISCUSSION

The patient studies in this article demonstrate the utility of intraprocedure 3D guidance and imaging during endovascular procedures. Three-dimensional RA acquisitions provide accurate anatomical information and advanced quantitative analysis tools, multimodality matching, and 3D navigation; soft tissue imaging can then be routinely used in synergy with 2D imaging to achieve improved clinical outcome and faster procedural workflow for a variety of applications. Our results suggest that 3D tools have clinical scope, particularly in optimal 3D viewing and navigation of tortuous and highly bifurcating vascular networks such as renal, hepatic, uterine, and external iliac arteries and veins. Three-dimensional runs also allow fast selection of favorable working projections during the embolization of aneurysms, AVMs, tumors, and uterine fibroids, and in a comprehensive treatment planning and evaluation
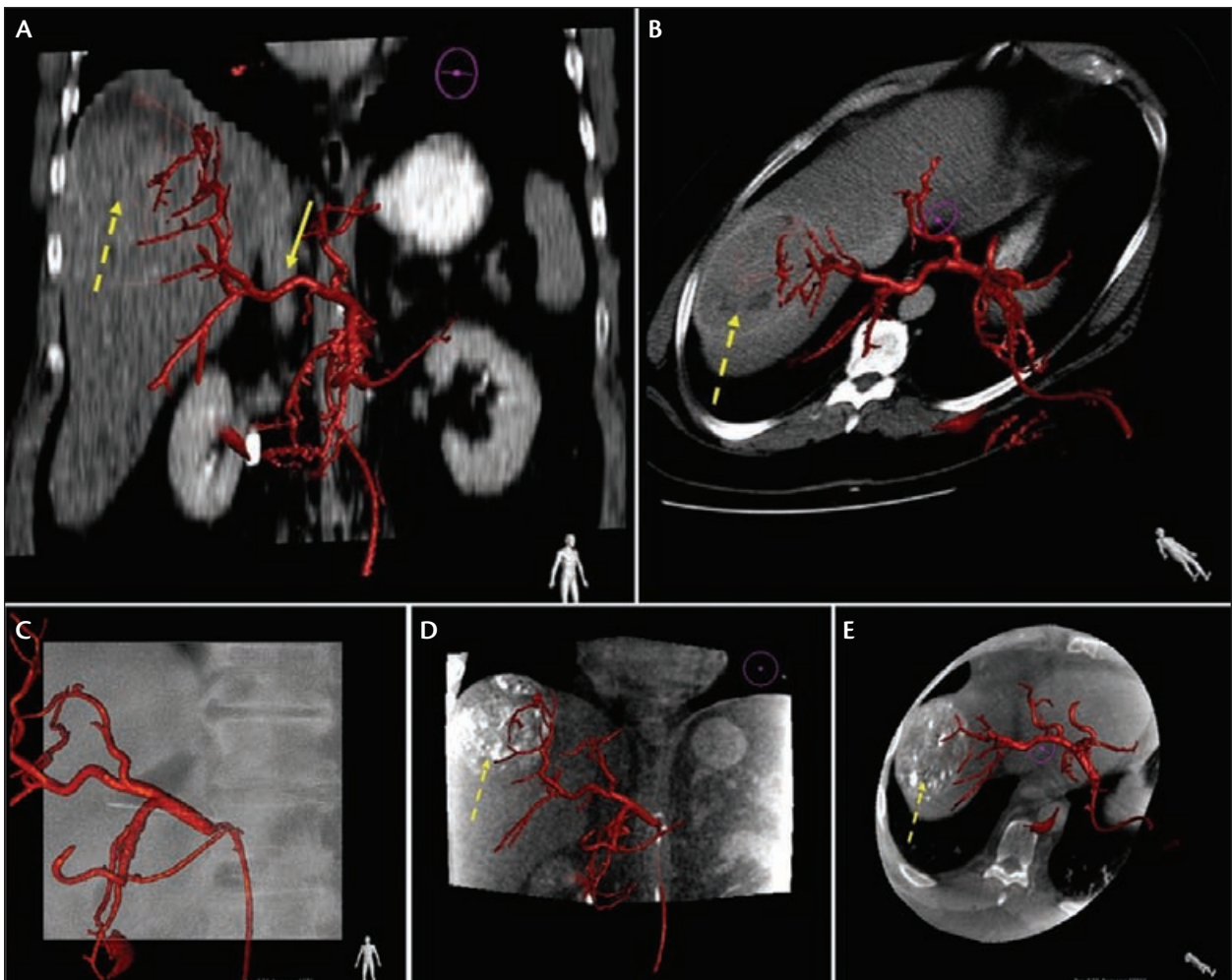
Figure 10. A TACE in a 67-year-old man affected by hepatocellular carcinoma. Multimodal reconstruction of common hepatic artery supply (arrow) from 3D RA surface rendering superimposed upon CT acquired before treatment. A globe-like tumor (dashed arrow) is shown in the right lobe of the patient's liver (A and B). Snapshot recorded during live navigation with Dynamic 3D Roadmap. Although breathing artifacts can make the use of 3D information difficult, the Dynamic 3D Roadmap still provided enough detail to achieve an adequate positioning of the catheter at the origin of the arterial supply prior to embolization (C). Posttreatment XperCT showing complete embolization of liver tumor (dashed arrow) (D and E). The intratumor enhancement due to the iodinated embolic material was validated throughout the entire tumor volume, thus confirming a technically successful TACE procedure.

with detailed visualization of devices and soft tissue in CT-like imaging (which is particularly useful in oncologic TACE procedures). In addition, the fact that a full 3D acquisition can now be obtained in a matter of seconds (approximately 4 seconds with the system and settings used in our institution) makes 3D RA readily available for all cases involving a number of initial unsuccessful attempts during navigation and/or embolization based on 2D imaging. Other potential endovascular applications not considered here but reported in the literature include anatomical visualization during aortic endograft procedures, evaluation and follow-up imaging of trans-

planted kidneys, and the evaluation of pancreas allografts.[13-15]

An optimal combination of 2D and 3D imaging may also lead to a reduction of radiation dose and contrast administration during endovascular procedures. Although quantitative studies should be pursued to evaluate procedure-based benefits of 3D RA, the use of a single 3D RA for 3D road mapping and for pretreatment selection of optimal working projections showed clear potentials for cases requiring multiple oblique 2D DSA runs and injections. It should be noted that, although 3D RA series involve a larger number of

images, depending on the exposed anatomical region, a single 3D RA image requires a dose that is 10 to 80 times lower than a single 2D DSA image.[9] This means that a 3D RA scan is equivalent to less than 4 seconds of a 2D DSA acquisition at 3 frames per second. A recent multicenter comparison has shown that the use of 3D RA for carotid artery treatment involves a cumulative radiation dose three times lower than for procedures based on 2D angiography only, mainly due to quicker selection of working projections and consequent reduction in fluoroscopy time and number of 2D DSA series.[10]

A correct combination of 2D and 3D information is also essential to support the interventionist in the deployment of new minimally invasive procedural approaches. For example, the recent combination of fluoroscopy and 3D imaging in an integrated tracking and navigation system has allowed interventional radiologists to achieve live 3D guidance in the interventional suite and to open new application areas for deep injections, biopsies, and drainages.[16] Intraprocedure 3D information also allows for a smooth integration of CTA and MRA diagnostic data in the interventional workflow and is essential for the introduction of advanced modeling and simulation technologies.[17] Further technology development should focus on the compensation of motion artifacts affecting the integration of live 2D and 3D imaging, with the potential of extending the usability and application range of 3D tools in endovascular procedures.

Vendors of angiography systems offer competing versions of the 3D interventional tools mentioned in this article, which go by names like Innova 3D and Innova CT (GE Healthcare, Chalfont St. Giles, United Kingdom); syngo InSpace 3D, DynaCT, iPilot, and iGuide (Siemens Healthcare, Erlangen, Germany); Allura 3D RA, XperCT, Dynamic 3D Roadmap, and XperGuide (Philips Medical Systems); and 3D Angio (Toshiba Medical Systems Corporation, Tokyo, Japan). These vendors' 3D packages do vary significantly in their speed of acquisition, image quality, feature set, reconstruction times, and ease of use. We encourage the interventionist to carefully compare the various vendors' 3D technologies when choosing an angiography system, because we expect the use of these 3D tools to significantly increase and be an integral part of future interventions.

CONCLUSION

The availability of 3D tools is indispensable in a busy day-to-day endovascular practice and promotes good clinical outcome and efficient procedural workflow. We encourage the use of 3D tools to achieve fast, accurate,

and confident decisions with a potential reduction in contrast administration and radiation dose to patients and staff. ■

For videos associated with this article, please visit the July 2009 issue of *Endovascular Today* at evtoday.com.

Atul Gupta, MD, is the Director of Interventional Radiology at Paoli Hospital, Main Line Health, in Paoli, Pennsylvania. He has disclosed that he is a member of the Medical Advisory Board for Philips Healthcare. Dr. Gupta may be reached at (610) 648-1255; guptaa@mlhs.org.

Alessandro G. Radaelli, PhD, is a clinical scientist (cardiovascular x-ray) employed by Philips Healthcare in Best, The Netherlands. Dr. Radaelli may be reached at +31 40 27 66685; alessandro.radaelli@philips.com.

1. Kakeda S, Korogi Y, Ohnari N, et al. Usefulness of cone-beam volume CT with flat panel detectors in conjunction with catheter angiography for transcatheter arterial embolization. J Vasc Interv Radiol. 2007;18:1508-1516.
2. Klucznik RP. Current technology and clinical applications of three-dimensional angiography. Radiol Clin North Am. 2002;40:711-728.
3. Seibert JA. Flat-panel detectors: how much better are they? Pediatr Radiol. 2006;36:173-181.
4. Willhelm K, Babic D. 3D angiography in the interventional clinical routine. MedicaMundi. 2006;50:24-31.
5. Anxionnat R, Bracard S, Ducrocq X, et al. Intracranial aneurysms: clinical value of 3D digital subtraction angiography in the therapeutic decision and endovascular treatment. Radiology. 2001;218:799-808.
6. Abe T, Hirohata M, Tanaka N, et al. Clinical benefits of rotational 3D angiography in endovascular treatment of ruptured cerebral aneurysm. AJNR Am J Neuroradiol. 2002;23:686-688.
7. Hochmuth A, Spetzger U, Schumacher M. Comparison of three-dimensional rotational angiography with digital subtraction angiography in the assessment of ruptured cerebral aneurysms. AJNR Am J Neuroradiol. 2002;23:1199-1205.
8. Racadio JM, Fricke BL, Jones B, et al. Three-dimensional rotational angiography of neurovascular lesions in pediatric patients. AJR Am J Roentgenol. 2006;186:75-84.
9. Schueler BA, Kallmes DF, Cloft HJ. 3D cerebral angiography: radiation dose comparison with digital subtraction angiography. AJNR Am J Neuroradiol. 2005;26:1898-1901.
10. Tsapaki V, Vano E, Muavrikou I, et al. Comparison of patient dose in two-dimensional carotid arteriography and three-dimensional rotational angiography. Cardiovasc Intervent Radiol. 2008;31:477-482.
11. Bozlar U, Edmunds JS, Turba UC, et al. Three-dimensional rotational angiography of the inferior vena cava as an adjunct to inferior vena cava filter retrieval. Cardiovasc Intervent Radiol. 2009;32:86-92.
12. Naguib NNN, Nour-Eldin NEA, Hammerstingl RM, et al. Three-dimensional reconstructed contrast-enhanced MR angiography for internal iliac artery branch visualization before uterine artery embolization. J Vasc Interv Radiol. 2008;19:1569-1575.
13. van den Berg, JC. Radio-anatomy of the thoracic aorta: 3D imaging of the aorta (CT, MRI and 3D rotational angiography). In: Rousseau H, Verhoye J-P, Heautot J-F, eds. Thoracic Aortic Diseases. New York, NY: Springer Berlin Heidelberg; 2006:3-19.
14. Hagen G, Wadstrom J, Magnusson A. 3D rotational angiography of transplanted kidneys. Acta Radiol. 2003;44:193-198.
15. Bozlar U, Brayman K, Hagspiel K. Pancreas allografts: comparison of three-dimensional rotational angiography with standard digital subtraction angiography. J Vasc Interv Radiol. 2008;19:239-244.
16. Racadio JM, Babic D, Homan R, et al. Live 3D guidance in the interventional radiology suite. AJR Am J Roentgenol. 2007;189:357-364.
17. Bullitt E, Aylward S. Visualizing blood vessel trees in three dimensions: clinical applications. Presented at: Medical Imaging 2005: Image Perception, Observer Performance, and Technology Assessment; February 15, 2005. doi: 10.1117/12.604746.